International Journal of
Turbomachinery
Propulsion and Power

MDPI

Article

Hot Streak Evolution in an Axial HP Turbine Stage †

Paolo Gaetani * and Giacomo Persico

Laboratorio di Fluidodinamica delle Macchine, Dipartimento di Energia, Politecnico di Milano, Via Lambruschini, 4, 20158 Milano, Italy; giacomo.persico@polimi.it

* Correspondence: paolo.gaetani@polimi.it; Tel.: +39-2-2399-8614

† This paper is an extended version of our paper in Proceedings of the European Turbomachinery Conference ETC'12, 2017, Paper No. 182.

Academic Editor: Marcello Manna
Received: 24 March 2017; Accepted: 18 April 2017; Published: 27 April 2017

Abstract: This paper presents the results of an experimental study on the evolution of hot streaks generated by gas turbine burners in an un-cooled high-pressure turbine stage. The prescribed hot streaks were directed streamwise and characterized by a 20% over-temperature with respect to the main flow at the stage inlet. The hot streak was injected in four different circumferential positions with respect to the stator blade. Detailed temperature and aerodynamic measurements upstream and downstream of the stage, as well as in-between the blade rows, were performed. Measurements showed a severe temperature attenuation of the hot streaks within the stator cascade; some influence on the aerodynamic field was found, especially on the vorticity field, while the temperature pattern resulted in severe alteration depending on the injection position. Downstream of the rotor, the jet spread over the pitch above the midspan and was more concentrated at the hub. Rotor secondary flows were also enhanced by hot streaks.

Keywords: hot streaks; axial turbine; turbine performance; combustor-turbine coupling

1. Introduction

The optimization of a gas turbine engine is crucially influenced by the combination between the combustor and the high pressure turbine (HPT). The progressive rise in turbine inlet temperature and the subsequent lower dilution ratio, the reduction of engine axial length and the increased loading of the turbine blades make the combustor-turbine matching critical, resulting in aero-thermal [1–4], as well as aero-acoustic [5], issues. The HPT is characterized by inlet total temperature distortions due to the residual traces of the combustor burners, which are normally called 'hot streaks'. Theoretical analyses [6,7] suggested that the migration of hot streaks in stationary and rotating blade rows should occur according to different mechanisms. In particular, the hot streaks incoming in the turbine stage should be convected throughout the stator channel to be finally released as high-speed jets, which impinge on the rotor blade pressure side and cause a periodic fluctuation of the rotor incidence angle. These features might significantly alter the blade surface temperature, with noteworthy implications on the rotor cooling effectiveness [2]. In addition to detailed investigations on the aerothermal features of the flow released by combustors ([8], among others), recent studies have considered more realistic configurations, combining the hot streak with a local streamwise vorticity [9] and studying the potential for clocking between the burners and the stator blades [10]. The residual hot streak entering the rotor induces even more complex features within the rotor blade row, including the generation of further vorticity cores which are pushed towards the endwalls [11], altering the wall temperature in these regions and triggering the development of novel cooling techniques [12]. These studies suggest that the evolution of the hot streaks within the two cascades involves complex phenomena, which also have relevant effects on the aerodynamics of the HPT; they indicate the need of further experimental

studies for a proper understanding of the phenomena involved. To this end, an experimental and computational study on hot streak evolution in a HPT has been recently launched at Politecnico di Milano. This paper presents the results of the first experimental campaign on hot streak migration in the stator and in the rotor of an HPT model, for four different clocking positions between the hot streak and the stator blade, thus providing a unique dataset for flow analysis and computational model assessment.

2. Test Rig and Instrumentation

2.1. Test Rig

Measurements were performed in the high-speed closed-loop test rig of the Laboratorio di Fluidodinamica delle Macchine (LFM) of the Politecnico di Milano (Italy). The facility is conceived so that a centrifugal compressor and a cooler provide the flow rate and the incoming conditions for the test section, where a single-stage, engine-representative HP turbine is installed. Full details on the facility and the research turbine can be found in [13]. Table 1 provides relevant information on the turbine geometry, as well as the reference operating conditions of the present tests. For this first study on hot-streak migration in the turbine, subsonic conditions were considered (even though measurements in transonic conditions have been recently published in [14]). The aerodynamics of the turbine operated in subsonic conditions was extensively studied in the last decade and can be found in [15–17]. Briefly, under the expansion ratio of 1.4, the flow condition is subsonic for both the stator and the rotor; to set a reference, the stator outlet Mach number at the midspan is 0.6 and the Reynolds is 9×10^5, based on the stator chord. As an average, the rotor outlet relative Mach number is 0.45 with a Reynolds number of 5×10^5, based on the rotor chord. A meridional cut of the test section is provided in Figure 1, which also shows the turbine inflow system, composed of an inlet centripetal guide vane and a straightener (honeycomb), followed by a 400 mm long annular duct upstream of the turbine. Within this duct, two vane axial chords upstream of the vane leading edge, an injector row was installed to simulate the (steady) hot streaks produced by the gas turbine burners; to impose a simple azimuthal periodicity, one injector out of two stator blades was installed (overall, 11 injectors).

The present hot streak generator (HSG) was derived from the entropy wave generator (EWG) developed for indirect combustion noise experiments and presented in [18]. For the purposes of the present experiment, the hot streak is generated by injecting a steady stream of hot air in mechanical equilibrium with the surrounding flow. The selection of the feeding pressure to ensure the optimal injection of the hot flow within the main stream was made after a wide preliminary experimental study on the turbine incoming flow, documented in [18,19]. The injection temperature was the maximum achievable with the present HSG device, as will be discussed in detail later. The device was allowed to reach 390 K in the core of the hot streak, as measured on a traverse placed one vane axial chord upstream of the vane leading edge. This temperature peak corresponds to an increase of 20% of the main stream temperature, which is a realistic representation of hot-streak-induced temperature perturbation; just to set a general context, [9,12] documented a temperature ratio of ~1.09 while [8,10] imposed a ratio greater than 1.5. The hot streaks were injected at 70% of the span in the stream-wise direction, with the aim of minimizing the injector blockage and of limiting the jet interaction with the vane secondary flows. Injectors themselves, create a weak blockage to the turbine mass flow but, thanks to the injected mass flow (which amounts to ~1% of the main stream one), the overall impact of the injection on the mass flow was negligible.

Table 1. Laboratorio di Fluidodinamica delle Macchine high-pressure turbine stage geometry.

Op. Cond.	**β**	***n* (rpm)**	***G* (kg/s)**	$T_{T,IN}$ **(K)**
	1.4	7000	3.78	323
Geometry	***h* (mm)**	t_c/h	D_M **(mm)**	$gap/c_{x,V}$
	50	0.02	350	1.00
Blade Rows	N_b	σ	***AR***	**Δ*θ***
Vane	22	1.20	0.83	75.2
Rotor	25	1.25	0.91	115.3

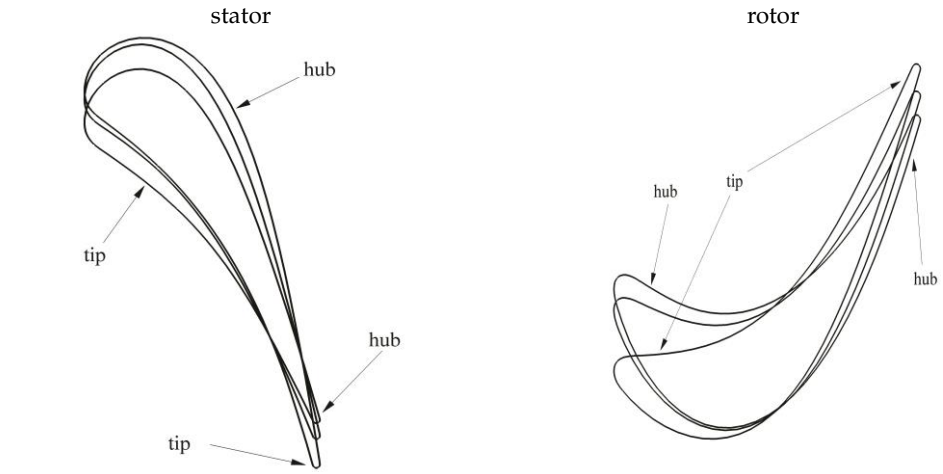

See nomenclature for definitions.

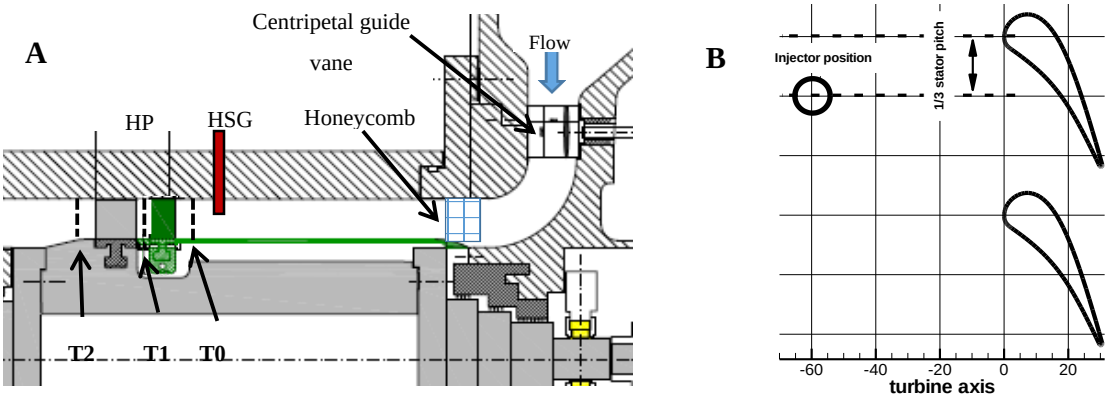

Figure 1. (**A**) Meridional cut of the test section; T0 = stator upstream traverse; T1 = stator downstream; T2 = rotor downstream; HSG, hot streak generator; HP, high pressure stage; (**B**) Injector to stator vane position for the pressure side case test point.

2.2. Instrumentation

The experiments documented in this paper were performed by applying a combination of conventional techniques, namely thermocouple and pneumatic probes, with fast-response aerodynamic pressure probes (FRAPP). The turbine inlet flow was measured with a flattened total pressure probe (designed and manufactured in-house, probe head dimension 0.5 mm, uncertainty = 60 Pa) and a hot wire probe (Dantec, Skovlunde, Denmark), both traversed spanwise one and a half stator axial chords upstream of the stage; in this section a flat profile of uniform total pressure and 2.5% of turbulence intensity were found between 20% and 80%.

Three-dimensional time-averaged flow measurements downstream of the stator were performed with a five-hole pneumatic probe (5HP, designed and manufactured in-house), which features a 1.4 mm head dimension. The probe was placed 32% of the stator axial chord downstream of the stator trailing edge. The 5HP was calibrated in a reference nozzle up to transonic conditions, exhibiting uncertainty of 0.2° in the flow angles and, as a maximum, of 0.5% of the local kinetic head for pressures; the uncertainty of the total pressure loss coefficient is 0.2%.

The unsteady flow field downstream of the rotor was measured by a cylindrical single-sensor FRAPP (designed and manufactured in-house) at an axial distance of 32% of the rotor axial chord downstream of the trailing edge. The FRAPP was statically calibrated both in pressure and temperature in order to compensate for any thermal drift during the measurement campaign. FRAPP was operated in a virtual three-sensor mode and, by applying an ensemble averaging in post-processing, the phase-resolved components of flow angle, total pressure, and Mach number were measured. The probe was calibrated up to Mach = 0.8 in a reference nozzle resulting in uncertainty of 0.25° on the flow angles and 0.5% of the kinetic head for the pressures. More details on the FRAPP technology can be found in [20]. Dedicated dynamic calibration showed a dynamic response of ~80 kHz after digital compensation [21].

The time-averaged temperature fields were measured by a conventional K thermocouple (joint diameter = 0.25 mm, Tersid Srl., Milan, Italy) inserted into a vented probe. The axial positions of the temperature traverse coincide with those pertaining to the 5HP and the FRAPP. The thermocouple was calibrated in a reference oven, resulting in an uncertainty of 0.3 K. Dedicated tests in a calibrated nozzle showed, over the Mach number range of interest, a substantial invariance of the probe temperature measurement with the flow angle and a recovery factor close to unity.

Due to mechanical constraints on the turbine casing, probes could be traversed only for one stator pitch in the tangential direction. This did not turn out to be a penalty for the investigation of the flow upstream and downstream of the stator, because the hot streak evolution remained confined in a single vane passage, as described in the following. On the contrary, it was not possible to investigate the full periodicity over 1/11 of the annular crown downstream of the rotor.

2.3. Test Matrix

In order to track the hot streak evolution for different azimuthal injection positions, the stator to injector position was varied. Four cases were studied, as reported in Table 2.

Table 2. Test matrix.

Name	Hot Streak Azimuthal Position
LE	Aligned to the stator leading edge
PS	At 1/3 of the pitch close to the pressure side
MP	At mid-pitch
SS	At 1/3 of the pitch close to the suction side

3. Results

In this section the results of the wide experimental campaign on the injector to stator clocking in the different axial positions of the machine will be presented and discussed.

3.1. Stator Inlet Conditions

The stator inlet conditions were measured for all four injector positions for assessment reasons; however, the large distance between injectors and the vane was sufficient to nullify the impact of the stator on the generation of the hot streaks, with identical results for all of the cases.

Figure 2 reports the total temperature and total pressure fields upstream of the stator when the hot streak is injected. As the present HSG is based on injection, no hot streak can be generated without

a dynamic pressure perturbation. So far, the injector wake and the hot streak produce a non-uniformity in the total pressure distribution (Figure 2B) which, however, results in a negligible variation of the stage pressure ratio. The temperature ratio between the core of the hot streak and the main stream is 1.2; as is visible in Figure 2A, the hot streak has an almost circular pattern that smooths down to the main stream temperature.

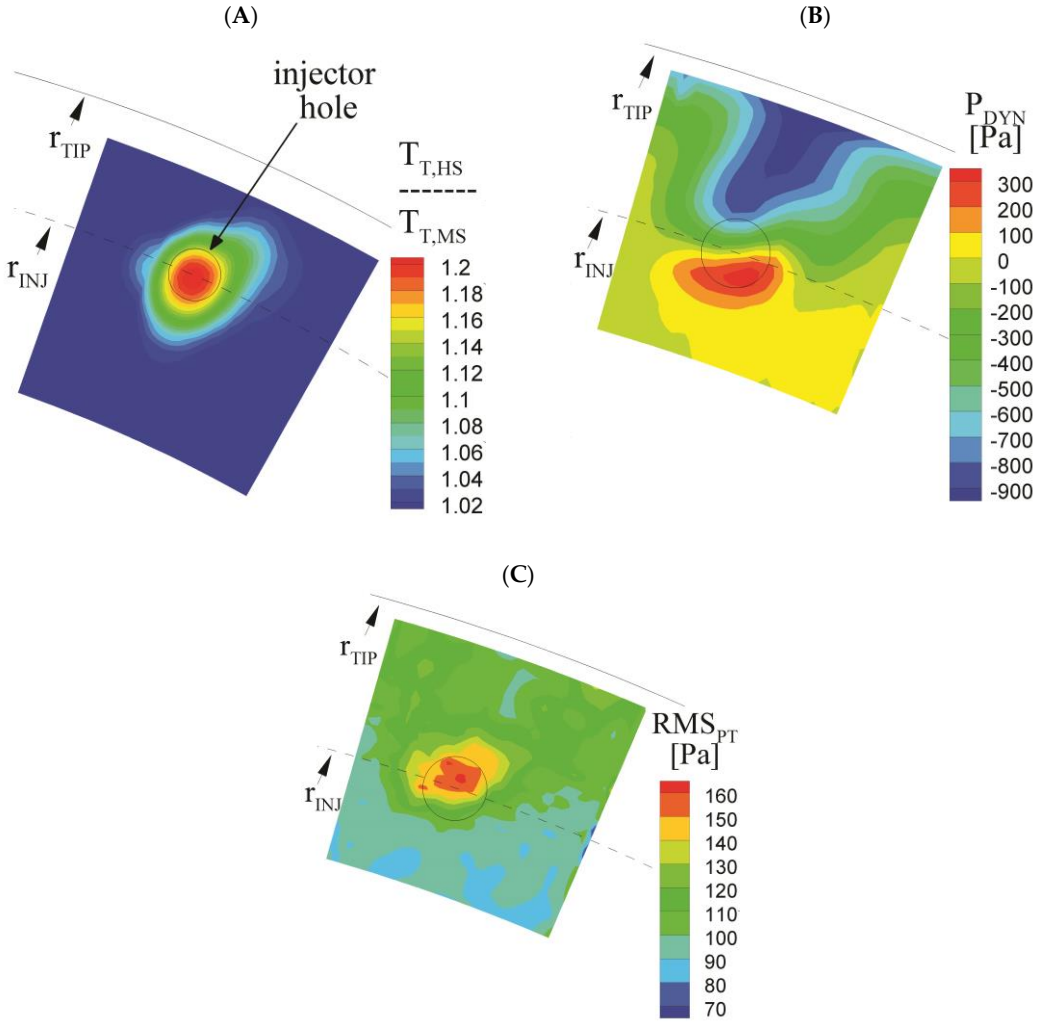

Figure 2. Total temperature (**A**), and total pressure (**B**) fields of the hot streak. Pmean is reported as a difference between the local total pressure and the main stream pressure (kinetic head = 1100 Pa). (**C**) RMS of the total pressure.

The RMS of the total pressure (Figure 2C) evidences the turbulent content of the hot streak, which results from the interaction of the jet with the surrounding flow and from the injector wake itself. The peak of the RMS is located at the upper boundary of the jet where the maximum total pressure gradient is found, namely where the largest shear layer establishes between the injector wake and the hot streak.

3.2. Stator Outlet Field

The stator-exit flow and thermal fields were investigated in dedicated and different tests, after a satisfactory repeatability in the operating condition was assessed. At first, an overview of the thermal field is provided by presenting the results for all four hot streak positions; then, the flow patterns are discussed in detail and compared in order to show the specific features of each case.

The total temperature field for the different cases is reported in Figure 3; a significant distortion was measured depending on the interaction between the hot streaks and the stator aerodynamics. Moreover, a severe temperature reduction, from 1.2 to 1.05 of the main stream total temperature, is found as a result of the heat exchange with the surrounding flow (and possibly with the blade) and of the diffusion due to turbulence and whirling flows inside the blade channel. For the LE case (Figure 3A), the hot streak directly impinges on the stator blade leading edge; the blockage imposed by the blade makes the high-temperature zone spread along the blade surface all across the span. In addition, the hot streak undergoes a stretching on the blade suction side (in all panels of Figure 3, it is located on the right-hand side of the wake trace) as a consequence of the acceleration and successive deceleration in the blade channel. It is also of interest to note that a temperature increase is found on the tip region towards the suction side of the adjacent blade (top-left corner in each panel of Figure 3); such a feature has to be ascribed to the interaction between the hot streak (or, at least, its portion convected on the pressure side of the blade surface) and the cross-flow connected to the tip passage vortex, that moves part of the hot streak flow along the casing. For the MP case (Figure 3B), the hot streak partially interacts with the wake and appears spread over a wide portion of the stator channel. An interaction with the secondary flow is still visible, although much weaker than in the LE case.

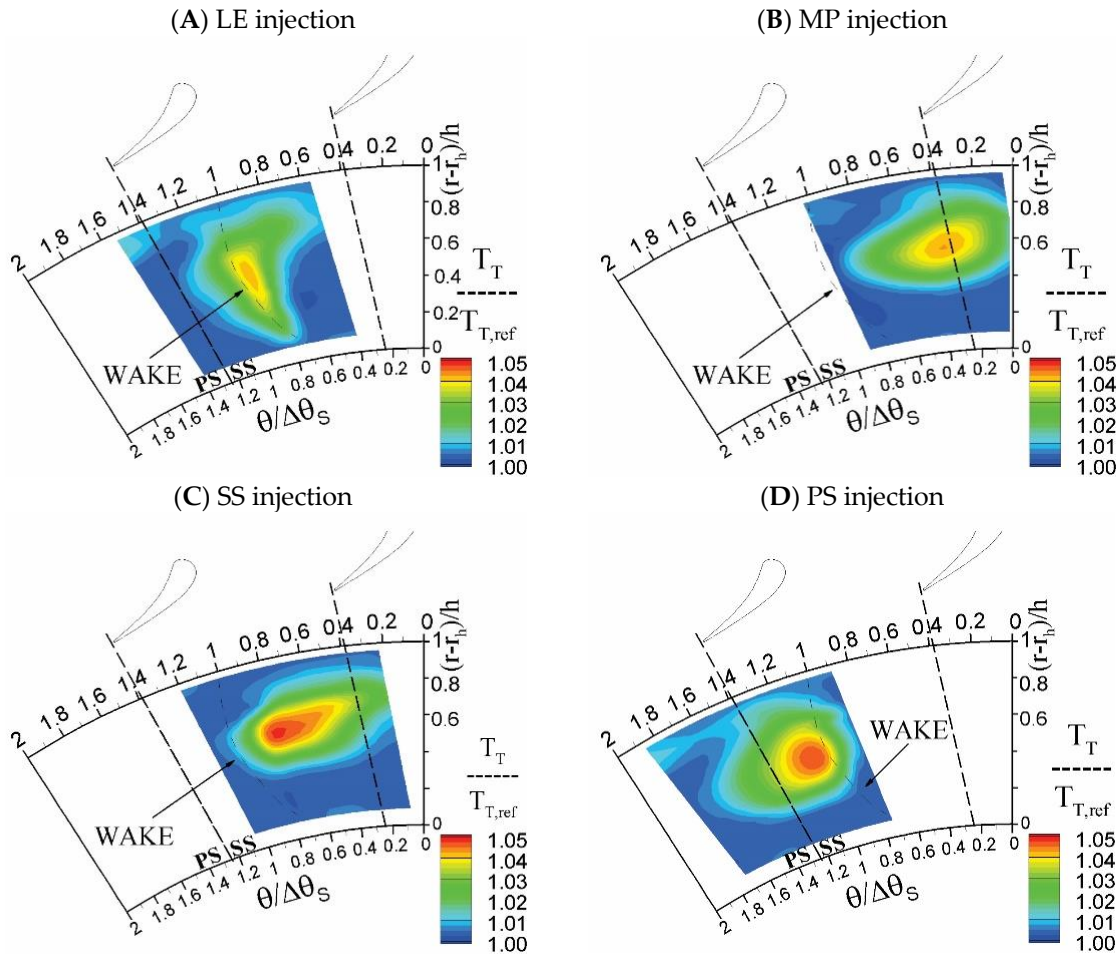

Figure 3. Total temperature fields downstream of the stator for the four hot streak positions.

A slightly higher preservation of the hot streak, resulting in a higher temperature peak, is found when the injection occurs close to the suction and pressure side (SS and PS cases, respectively in Figure 3C,D). For the PS case, the entrainment of the hot-streak in the wake and in the cross-flow of the passage vortex is of some importance. Despite the proximity to the wake, it seems that the wake

acts as a boundary to the hot streak diffusion. The SS case does not show any peak close to the casing. In fact, the interaction with the passage vortex seems to mainly occur with the under-turning side of the vortex, which is closer to the midspan: as a result, the hot area is stretched toward the pressure side of the adjacent blade.

In addition to the tangential displacement, the hot core is also shifted in the radial position, as shown in Figure 4, where the upstream profile is also reported. This feature depends on the stator leaning (about 10 degrees towards the pressure side): specifically, in the PS case, the hot streak is pushed toward the hub whereas, in the SS case, it remains closer to the tip. The MP case is between them, while the LE case exhibits a completely different behaviour of the hot streak.

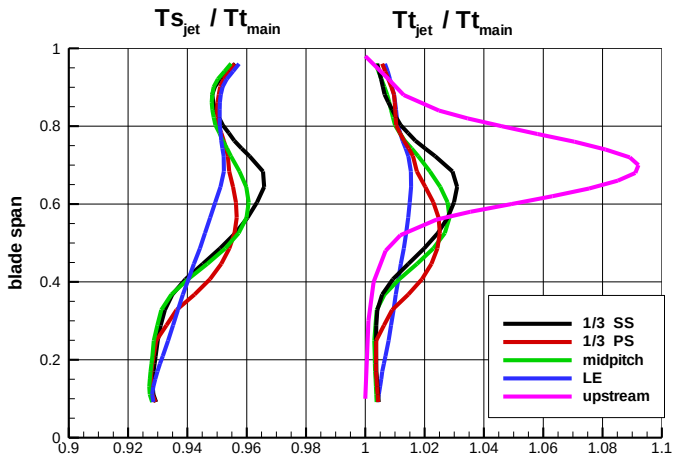

Figure 4. Static and total temperature pitch-wise averaged profile.

In addition to this description on the hot-steaks intensity and position, a more in-depth discussion and interpretation of the flow features for the different injection positions is reported below.

3.2.1. LE Injection Case

For this case, the strongest interaction between the jet and the blade has been highlighted. The impact of the hot streak on the blade wake can be observed in Figure 5, which reports the total pressure loss coefficient distributions for the reference and the hot streak conditions, as well as their difference; the wake retains its general width and deficit, even though a small tangential shift is found especially above the midspan. The stator-exit vorticity field, not reported for sake of brevity, does not show a specific effect of the hot streak on the stator secondary flow for LE injection (the reader is referred to [14] for a comprehensive discussion of the stator aerodynamics in the absence of hot streak injection). Overall, the hot streak injection slightly changes the cascade loss coefficient, especially above the midspan (namely, where the jet impinges on the blade), as reported in Figure 6. The tangential shift of the wake is, most probably, connected to the reduction in the mean angle along the blade span (about 1°), also visible in Figure 6, and especially in the radial position corresponding to the core of the hot streak. To assess the flow angle change and the local influence of the hot-streak, the difference in the flow angle between the hot case and the reference one is also reported in Figure 6. Such a change seems to be connected to the increase in the momentum at the stator exit and also implies a small reduction of the rotor incidence angle.

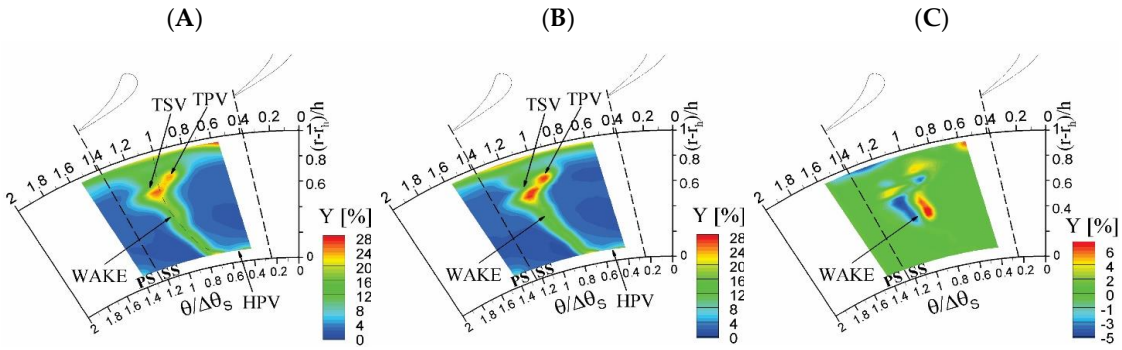

Figure 5. Total pressure loss coefficient at the stator exit for LE hot streak injection. (**A**) no injection; (**B**) with LE injection; and (**C**) point to point Y difference (hot streak—ref.). HPV, Hub Passage Vortex; TPV, Tip Passage Vortex ; TSV, Tip Shed Vortex.

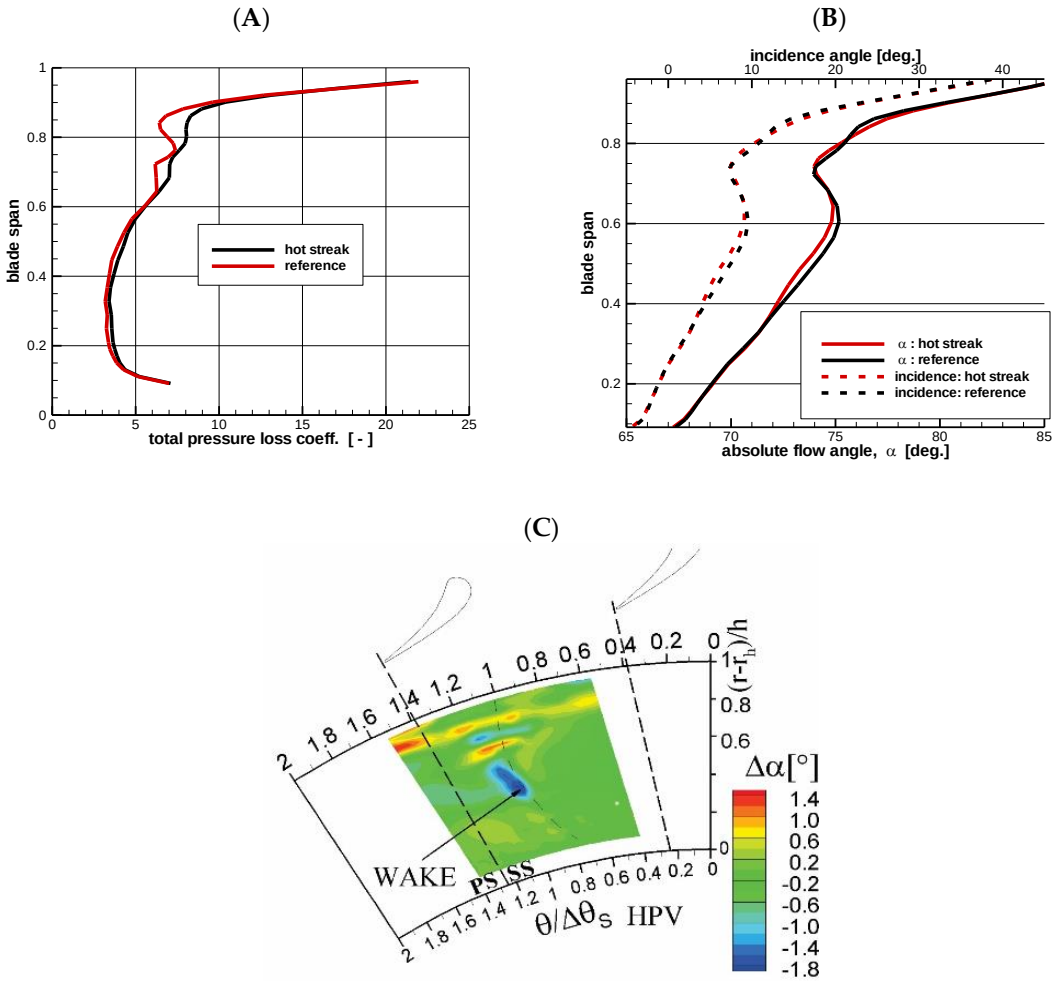

Figure 6. LE injection. (**A**) Y spanwise profile; (**B**) absolute flow angle and rotor incidence spanwise profiles; and (**C**) point-to-point flow angle difference, (hot streak—ref.).

3.2.2. MP Injection Case

A second important case is the mid-pitch injection: this is the case where the minimum interaction between the wake and the hot streak occurs. With reference to the loss coefficient distribution reported in Figure 7, the wake is almost unaffected by the hot streak; very small differences are found only at

the boundary of the wake. The pitch-wise averaged profiles, reported in Figure 8, further confirm such a conclusion by showing a very small loss increase only concentrated in the tip passage vortex region.

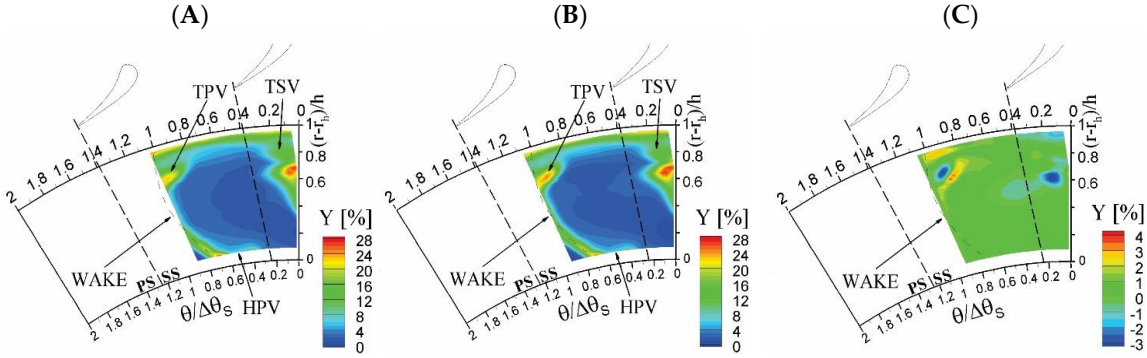

Figure 7. Total pressure loss coefficient at the stator exit for MP hot streak injection. (**A**) no injection; (**B**) with LE injection; and (**C**) difference, (hot streak—ref.).

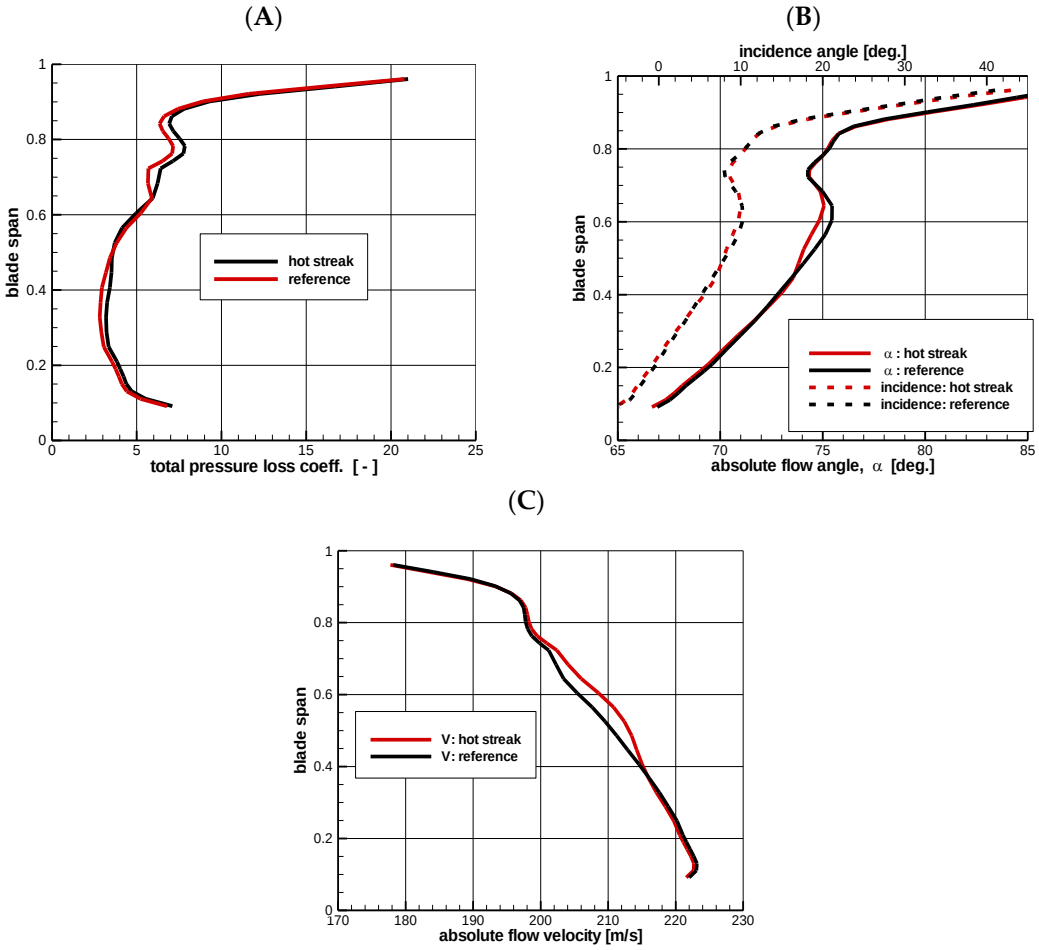

Figure 8. MP injection. (**A**) total pressure loss coefficient spanwise profiles; (**B**) absolute flow angle and rotor incidence spanwise profiles; and (**C**) absolute flow velocity spanwise profiles.

Thanks to the weak interaction with the wake, the hot streak causes some difference in the free-stream area, where a significant change in the flow angle is found between 40% and 70% of the blade span (Figure 8B). Such variation is induced by the increase in the velocity magnitude occurring in the hot streak with respect to the reference case, which is also well visible in Figure 8C (with a peak

difference of ~10 m/s): as a matter of fact, since the expansion ratio remains constant, any perturbation in the incoming total temperature field induces a velocity change. The change in the flow angle, which becomes more axial, combined with the concurrent increase in the velocity leaves the incidence angle on the rotor almost unchanged.

It is interesting to note that the incoming hot streaks trigger the onset of two additional vorticity cores in the stator-exit flow field at the top and bottom margins of the jet (which is roughly centred at 60% span), as visible in the streamwise vorticity fields reported in Figure 9. These features could be caused by the velocity gradients in the shear layer between the hot streak and the main stream, or by the total pressure gradients in the wake of the injector, that inevitably accompany the hot streaks in these experiments. The upper vorticity core enforces the tip shed vorticity while the lower one stands isolated as a flow structure crossing the whole pitch in the tangential direction. The enhancement of the shed vorticity also involves an increase of the vorticity in the boundary layer, this latter also being related to the injector wake.

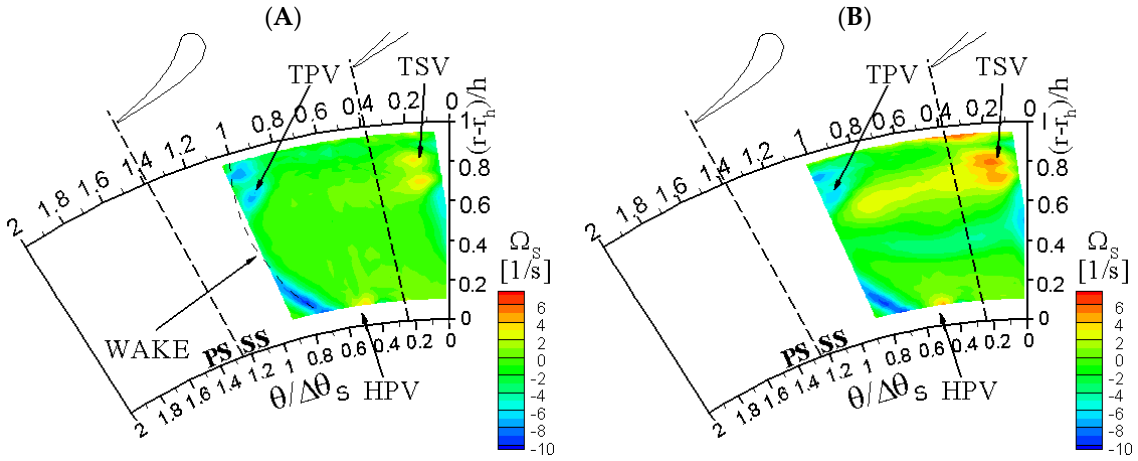

Figure 9. Streamwise vorticity in reference (**A**) and hot streak (**B**) cases for MP injection.

3.2.3. PS and SS Injection Cases

In the case of PS injection, the temperature distribution is similar to the one found for MP injection, although the hot streak is more concentrated and intense, as visible in Figure 3. The impact on the flow angle is also similar to that observed for MP injection, and slightly more intense. A peculiar pattern is found on the vorticity distribution, which is shown in Figure 10 alongside the corresponding reference case. The hot streak seems to induce, also for this case, a significant enhancement of the positive vorticity area (PV) on the pressure side of the wake (where the tip shed vortex (TSV) is also visible in the reference case). Moreover, as the hot streak is now closer to the wake with respect to MP injection, a more significant interaction with the wake occurs in the midspan region, which results in the onset of a local negative vorticity region (NV) at the hot streak bottom margin.

In the case of SS injection (Figure 11), the impact of the hot streak on the flow field exhibits the same features observed for the PS case; a similar amplification of the vorticity magnitude appears on the other side of the wake, in correspondence of the position of the hot streak. As a result, the vorticity pattern results are modified. To conclude, it is interesting to note that, except for the LE injection case, the hot streak (alongside the injector wake) induces a systematic effect on the flow field.

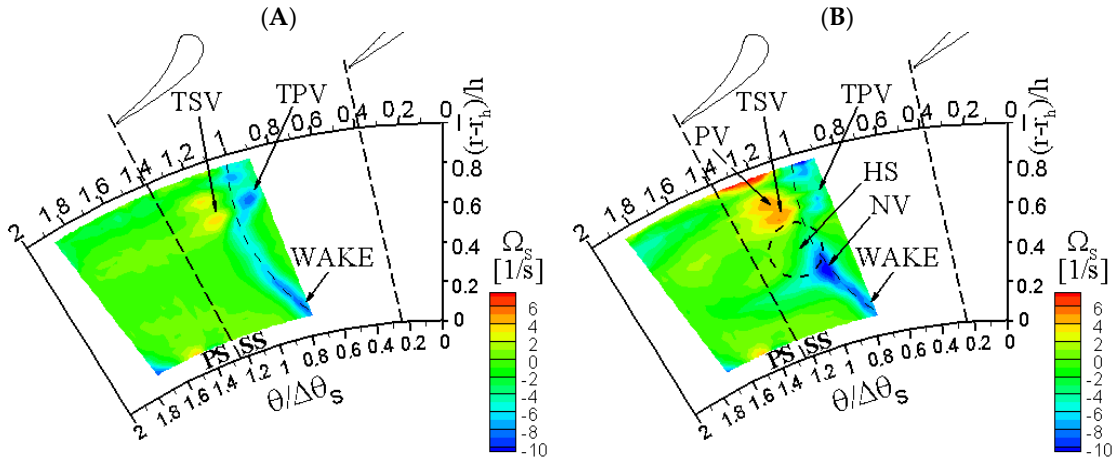

Figure 10. Streamwise vorticity in reference (**A**) and hot streak (**B**) cases for PS injection. HS, Hot Streak; NV, Negative Vorticity; PV, Positive Vorticity.

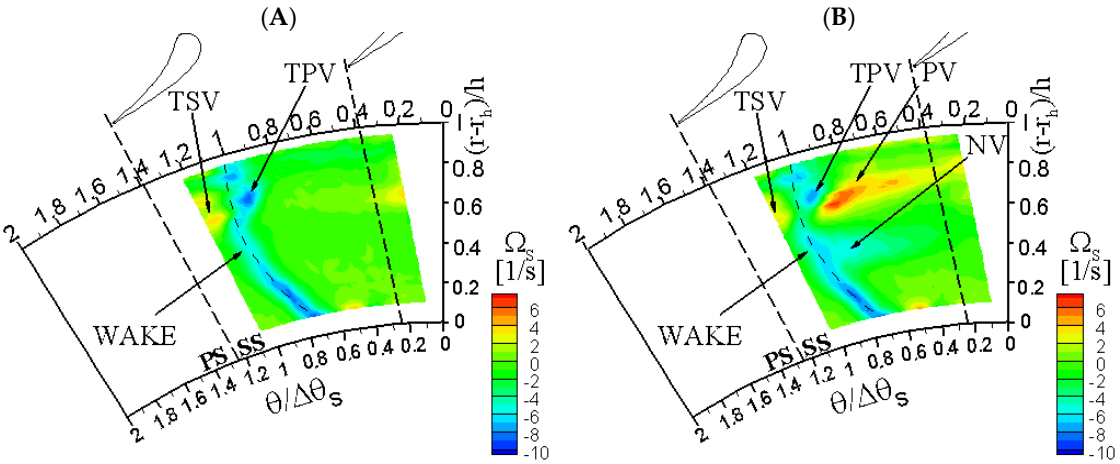

Figure 11. Streamwise vorticity in reference (**A**) and hot streak (**B**) cases for SS injection.

3.2.4. Stator Performance

The overall effect of the hot streak injection on the stator performance is weak for all four cases. In fact, given a total pressure loss coefficient of about 5.9% for the reference condition [14], the increase on the single stator channel (ΔY%) due to the hot streak injection is within 0.2% to 0.6%, as reported in Table 3, i.e., one order of magnitude lower and, for some cases, within the measurement uncertainty. The total temperature increase (ΔTt) is slightly changing with the minimum for the leading edge case, where the hot streak interacts directly with the blade and, for this, an effect of the heat exchange with the blade wall is expected, even though very difficult to quantify. The increment reported in Table 3 has to be compared with the mean total temperature increase at the stator inlet on the perturbed channel that is equal to 13.5 K, roughly three times of that found downstream of the stator.

The change in the kinetic energy, $\Delta(V^2/2)$, and in the momentum, $\Delta(\rho V^2/2)$, are also reported. The kinetic energy increases because of the higher total enthalpy available in the hot streak, and the highest magnitude is found on the pressure side where the hot streak undergoes lower mixing in the expansion process; on the contrary, the leading edge injection case exhibits the lowest value, due to the interaction with the blade. The momentum, instead, shows a decreasing trend when the hot streak is injected because of the change in the density related to the higher static temperature. The flow angle, given the high solidity is, in fact, negligibly affected by the hot streaks, its modifications being within the 5HP uncertainty.

Table 3. Overall parameter change downstream of the stator due to the hot streak injection: Δ = hot streak—reference flow conditions.

Position	ΔY%	ΔTt (°K)	$\Delta(V^2/2)$%	$\Delta(\rho V^2/2)$%
LE	0.45	3.9	0.3	−0.8
PS	0.24	4.9	1.5	−0.0
MP	0.32	4.5	0.9	−0.4
SS	0.59	4.7	0.4	−1.0

See nomenclature for definitions.

3.3. Rotor Outlet Field

In order to investigate the effects of the hot streaks on the whole turbine stage, the temperature field downstream of the rotor is now presented. By virtue of FRAPP measurements, the phase-resolved flow field was also measured and it is discussed below.

The reference flow field, which is representative for all the cases, was the object of a number of previous publications of the same group [17,22] and it is briefly recalled here.

3.3.1. Reference Time Mean Flow in the Rotating Frame

To properly discuss the stage-exit flow and temperature fields in the reference case, the time-averaged flow field in the rotating frame, derived from phase-resolved measurements, is first discussed. Figure 12 reports the relative total pressure coefficient (Cpt_R), rotor deviation angle (δ), and absolute flow angle (α) at the rotor exit. The Cpt_R map shows the rotor wake, identified as the region of the low total pressure coefficient, broadened and distorted by the secondary losses; the secondary flows are identified on the basis of the Rankine vortex model applied to the δ distribution. The tip region is dominated by the tip leakage vortex (TLV) and the tip passage vortex (TPV), while the midspan region shows a strong hub passage vortex (HPV) radially shifted by the inherent radial-outward migration of the passage vortices and by the Coriolis effect. The absolute flow angle shows an important flow deflection at the hub, mostly due to the cross-flow activated in the rotor blade row.

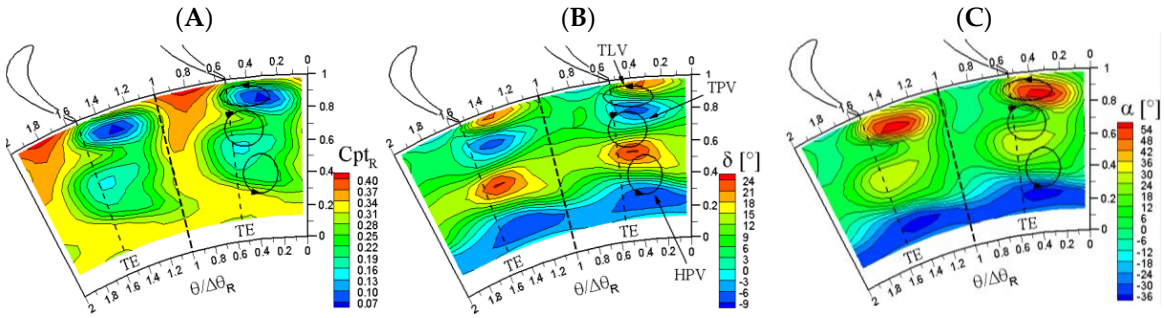

Figure 12. Time-mean flow in the rotating frame for the reference case. (**A**) total pressure coefficient, (**B**) deviation angle, (**C**) absolute flow angle

The time-averaged total temperature field at the stage exit for reference conditions (namely, without hot streak injection) is reported in the left frame of Figure 13. In the absence of upstream total temperature gradients, the distribution is dominated by the spanwise variation of work exchange. The flow experiences a reduction in the total temperature at the hub and close to the tip, in correspondence to the regions of higher work exchange connected to cross-flows and secondary flows. The wake avenue coming from the stator slightly alters the circumferential distribution of the work exchange, thus weakening the spanwise gradients in the central region of the pitch.

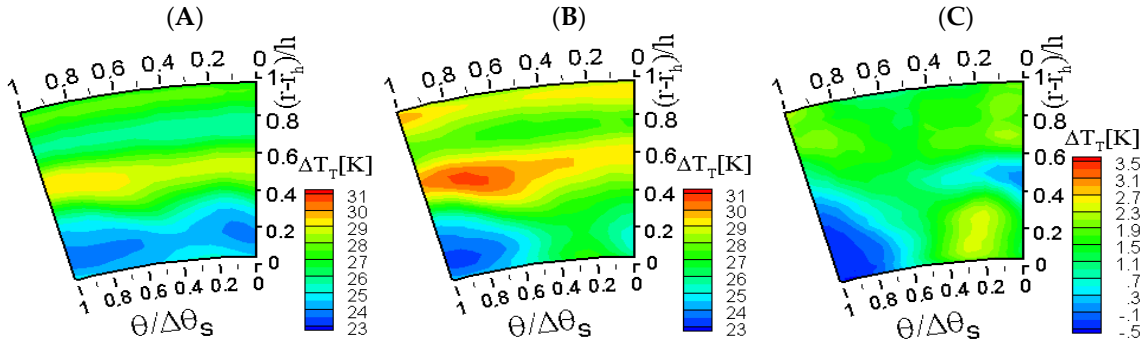

Figure 13. LE injection temperature field. (**A**) total temperature field in the reference condition; (**B**) total temperature field in the LE perturbed condition; and (**C**) point-to-point difference, (hot streak—ref.).

3.3.2. Temperature Field

When the hot streak is injected on the stator leading edge (Figure 13B), the hot fluid is entrained within the stator wake and, hence, high total temperature regions can be used as markers of the stator wake avenue at the rotor exit. To better highlight the traces of the hot streak, the difference between the two cases is considered and shown in Figure 13C. The hot streak appears to be spread all over the passage above midspan. At the hub, instead, it creates a hot spot whose extension is half of the passage, while the other portion experiences a weak decrease in the total temperature, suggesting an alteration in the work extraction process. The migration of the hot streak fluid towards the hub is probably promoted by the combined action of the radial equilibrium in the stator-rotor axial gap and of the rotor secondary flows on the stator wake. Figure 14 reports the results for the MP, SS, and PS cases. It is interesting to note that for all of these cases, and differently from what was observed in Figure 13, the hot streak appears somehow delimited to the upper part of the channel (namely, where the hot fluid is injected). It should be noted that the periodicity on one stator pitch is not anymore valid, as one injector out of two stator vanes was installed.

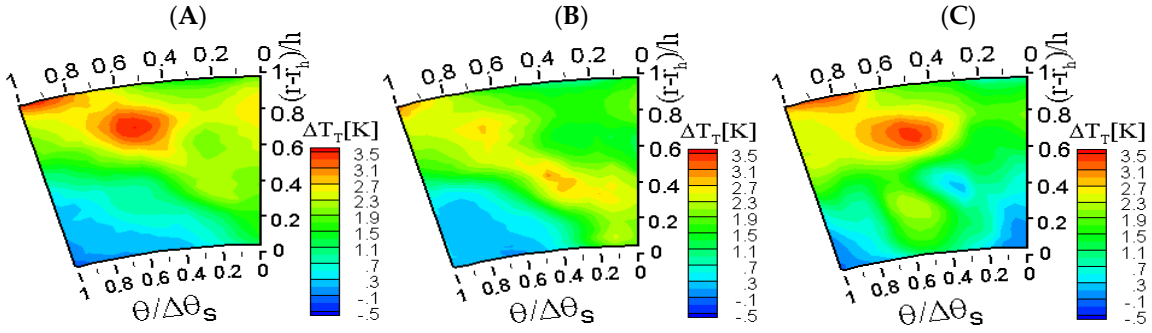

Figure 14. Point-to-point difference with respect to the reference case for: (**A**) MP injection; (**B**) PS injection; and (**C**) SS injection.

As previously described for the MP case, the hot streak location downstream of the stator was in the midspan-tip region and the additional induced vorticity combines with the rotor tip passage vortex one. These features lead to a hot streak spreading in the upper part of the channel with a weak influence on the hub region.

In the PS case, the core of the hot streak moved at the midspan of the rotor inlet (see Figure 4), and the hot fluid also interacts with the rotor hub passage vortex, leading to a stronger effect at the rotor hub. A contribution to the hot streak shift towards to hub may also come from its partial entrainment in the stator wake.

When the hot streak is injected close to the SS, it appears to split into two cores at the rotor exit, one close to the hub and the second one in the tip region. Such unexpected results depend on its position at the rotor entrance: likely, the hot streak portion located in the tip–freestream region is spread by the rotor secondary structures all over the rotor pitch, while the portion that was partially entrained by the wake it is now pushed—inside the rotor—by the centripetal pressure gradient towards the hub.

3.3.3. Time-Mean Flow Field in the Rotating Frame with Hot Streaks

Even though the impact of the hot streaks is mainly on the temperature field, some effects of small magnitude are also visible in the rotor aerodynamics, highlighted by FRAPP measurements.

In the presence of incoming hot streaks, the flow morphology is modulated depending on the injection position. As a general consideration, the hot streak strengthens and slightly shifts the rotor secondary flows, leading to changes in the flow angle distribution; conversely, negligible effects are detected on the pressure field and the Mach number distribution. Furthermore, as theoretically pointed out by [7], and computationally predicted by [11,12], the hot streak can alter the generation of the secondary vorticity in the rotor. For these reasons, the following analysis focuses on the experimental analysis of the rotor secondary flows and, hence, on the distribution of angles only.

As visible in Figure 15, which reports the point-by-point change between the reference case and those with the hot streak, the largest impact of the hot streak is measured for LE injection. Specifically, the effects of the LE injection consist in the strengthening of the tip leakage vortex and in a general reduction of the deviation angle in the midspan region, where the rotor hub passage vortex is found. This has a relevant impact on the absolute flow angle which increases, globally, above 60% of the span and reduces below the midspan. These features are probably correlated to the diffused and elongated shape of the hot streak entering the rotor, which result from the noteworthy interaction that establishes between the hot streak and the stator viscous structures in the case of LE injection.

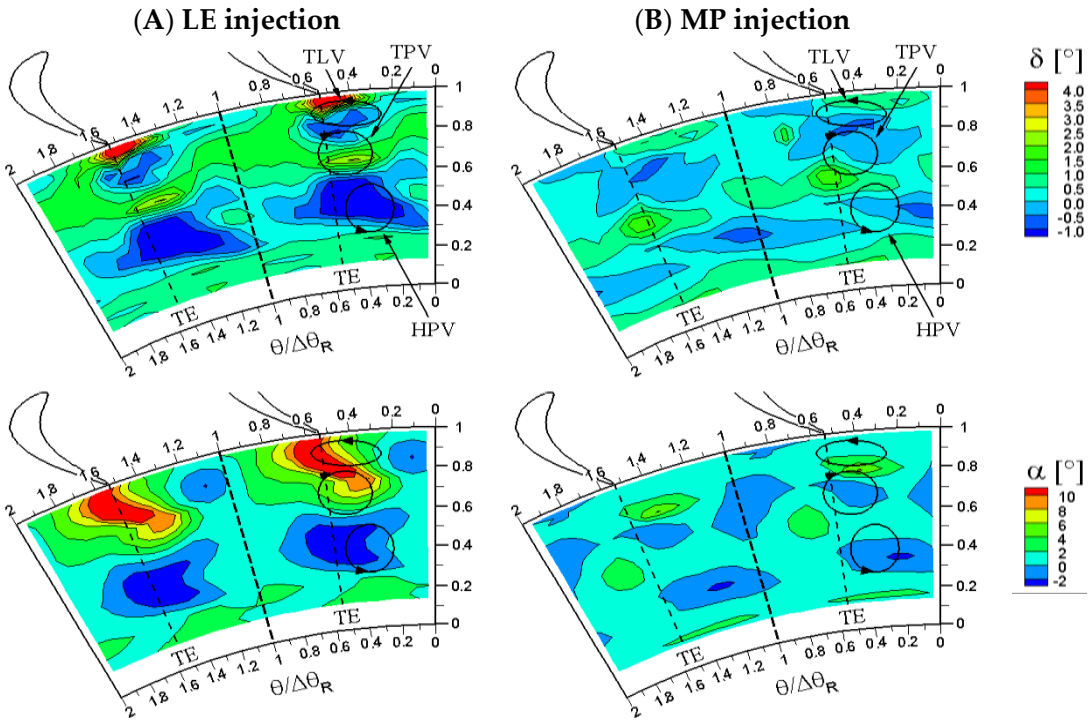

Figure 15. *Cont.*

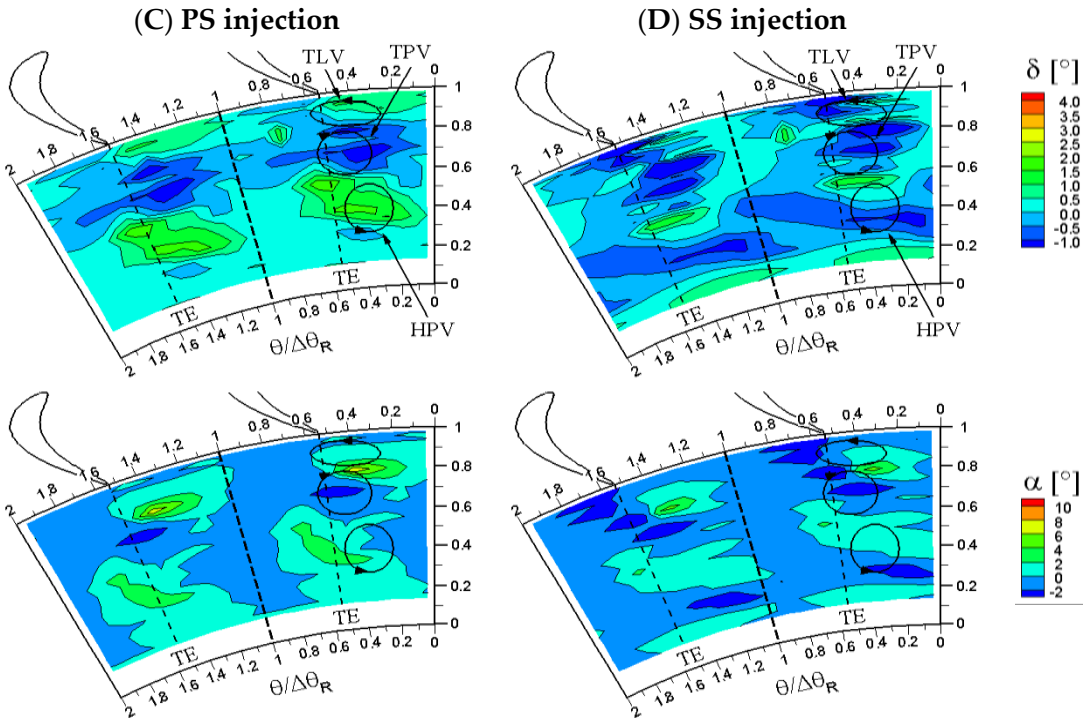

Figure 15. Point-to-point difference of mean flow angles with respect to the reference case. (**A**) LE injection; (**B**) MP injection; (**C**) PS injection; (**D**) SS injection.

The analysis of the other two cases, reported in t Figure 15C,D, confirms the impact of the hot streak position on the rotor secondary flows. In the PS injection case, the effect is also more intense downstream: the secondary flow pattern is slightly shifted below the midspan where a clear increase in the deviation angle is found. It is interesting to note that, in the passage vortex regions, the difference in δ measured for PS injection are similar to that observed for LE injection, even though opposite in sign. This is of some significance, considering that the LE injection has a negligible effect on the stator secondary flows, while the PS injection induces a relevant change in the stator-exit vorticity. In the case of SS injection, the minimum variation in the flow angle is found; this is consistent with the spreading of the hot streak over the entire passage observed on the basis of the temperature field (Figure 14C). Moreover, in this case, the stator outlet tip region was not affected, and for this is not energized by the hot streak, leading to a lower effect on the tip leakage vortex.

4. Discussion and Conclusions

The paper has presented a comprehensive analysis on the effect of hot streak migration within a high-pressure turbine. Hot streaks were injected in different clocking positions with respect to the stator blade, and provide a total temperature perturbation representative of aero-engine conditions. Several measurement techniques were applied to investigate the hot streak impact on the thermal and aerodynamic behavior of the stage.

It has been shown that, throughout the convection within the stator channel, the hot streak undergoes different migration and attenuation depending on the injection position. In particular, the clocking of the hot streak with the stator blade leading edge induces a dramatic deformation of the hot streak, which takes the shape of the blade wake. The temperature attenuation across the stator is severe for all the cases, and the maximum temperature ratio drops down from 1.2 to 1.05. With the exception of the injection on the suction side, a portion of the hot streak is entrained in the cross-flow induced by the stator pressure field on the shroud. A negligible increase in the stator total pressure loss is found due to the hot streak transport and evolution.

When the stator blade thermal stress is of concern, the hot streak injection on the leading edge is the worst possible operating condition, as can be argued by the temperature field downstream of the stator and as already pointed out by other authors [4]. The MP case seems to guarantee the lowest interaction with the blade and the highest temperature diffusion all over the channel. On the contrary, downstream of the rotor the highest diffusion is found for the PS injection, with potentially positive implications on the following stage.

The expected over-speed induced by the hot streak due to its higher enthalpy content at the stator exit is very limited, although expected also by theoretical analysis, as reported in [1], and has a minor impact on the rotor incidence angle. Conversely, an interesting effect is found on the vorticity field, which shows additional contributions at the top and bottom of the hot streak (except in the case of leading edge injection). Such additional vorticity cores also alter the rotor secondary flows as found at the rotor outlet. The temperature disturbance at the rotor outlet is further attenuated, consistently, with a significant spreading of the incoming rotor disturbances. These results are in line with the enhanced migration that the hot streak experiences in the rotating channel, and triggers the interest for further experimental and computational studies specifically oriented to the unsteady hot streak migration in the rotor. Due to the hardware limitations, hampering the flow field analysis over a 1/11 periodicity, no information can be drawn on the stage performance; such limits can be overcome by applying a computational fluid dynamic model, whose thorough validation is presently ongoing thanks to the wide set of data presented and discussed in this paper.

Acknowledgments: The present research is a follow up of the "REsearch on COrenoise ReDuction" (RECORD) project, grant agreement no. 312444, and funded by the European Union Seventh Framework Program (FP7/2007-2013).

Author Contributions: Paolo Gaetani is the leading author of this paper, having directed and contributed to all of the experiments, data reduction, and discussions reported in this paper. Giacomo Persico contributed to, and processed, the measurements at the rotor exit. The two authors equally contributed to the writing process of the paper.

Conflicts of Interest: The authors declare no conflict of interest.

Nomenclature

AR	aspect ratio
Cpt_R	relative total pressure coeff. $Cpt_R = \frac{Pt_R - Patm}{Pt_{in} - Patm}$
$c_{x,V}$	Vane axial chord
D_M	mean diameter
G	mass flow rate
h	blade height
HS	Hot Streak
HSG	Hot Streak Generator
Y	total pressure loss, $Y = \frac{Pt_{in} - Pt_{out}}{Pt_{out} - P}$
n	rotational speed
N_b	blade number
NV (PV)	Negative (Positive) Vorticity Core
r	radius
t_c	trailing edge thickness
TLV	Tip Leakage Vortex
TPV (HPV)	Tip (Hub) Passage Vortex
T_s	static temperature
TSV	Tip Shed Vortex
T_T	total temperature
V	absolute velocity
α	absolute flow angle, from axial
β	total to static expansion ratio
δ	deviation angle

σ	solidity
$\Delta\theta$	geometrical blade deflection
ρ	density
Ωs	streamwise vorticity
Subscripts	
h	hub
ref.	reference

References

1. Sharma, O.P.; Pickett, G.F.; Ni, R.H. Assessment of Unsteady Flow in Turbines. *J. Turbomach.* **1992**, *114*, 79–90. [CrossRef]
2. Butler, T.L.; Sharma, O.P.; Joslyn, H.D.; Dring, R.P. Redistribution of an Inlet Temperature Distortion in an Axial Flow Turbine Stage. *J. Propuls. Power* **1989**, *5*, 64–71. [CrossRef]
3. Dorney, D.J.; Sondak, D.L. Effects of Tip Clearance on Hot Streak Migration in a High Subsonic Single Stage Turbine. *J. Turbomach.* **2000**, *122*, 613–620. [CrossRef]
4. An, B.; Liu, J.; Jiang, H. Numerical Investigation on Unsteady Effects of Hot Streak on Flow and Heat Transfer in Turbine Stage. *J. Turbomach.* **2009**, *131*, 031015. [CrossRef]
5. Knoblock, K.; Neuhaus, L.; Bake, F.; Gaetani, P.; Persico, G. Experimental assessment of noise generation and transmission in a high-pressure transonic turbine stage. In Proceedings of the ASME Turbo Expo 2016: Turbomachinery Technical Conference and Exposition, Seoul, Korea, 13–17 June 2016.
6. Munk, M.; Prim, R.C. On the Multiplicity of Steady Gas Flows Having the Same Streamline Pattern. *Proc. Natl. Acad. Sci. USA* **1947**, *33*, 137–141. [CrossRef] [PubMed]
7. Hawthorne, W.R. *Secondary Vorticity in Stratified Compressible Fluids in Rotating Systems*; Report No. CUEDA-Turbo TR63; Department of Engineering, University of Cambridge: Cambridge, UK, 1974.
8. Andreini, A.; Bacci, T.; Insinna, M.; Mazzei, L.; Salvadori, S. Hybrid RANS-LES modelling of the aero-thermal field in an annular hot streak generator for the study of combustor-turbine interaction. In Proceedings of the ASME Turbo Expo 2016: Turbomachinery Technical Conference and Exposition, Seoul, Korea, 13–17 June 2016.
9. Jacobi, S.; Mazzoni, C.; Chana, K.; Rosic, B. Investigation of unsteady flow phenomena in the first vane caused by the combustor flow with swirl. *J. Turbomach.* **2017**, *139*, 041006. [CrossRef]
10. Koupper, C.; Bonneau, G.; Gicquel, L. Large eddy simulation of the combustor turbine interface: Study of the potential and clocking effects. In Proceedings of the ASME Turbo Expo 2016: Turbomachinery Technical Conference and Exposition, Seoul, Korea, 13–17 June 2016.
11. Giles, M.B.; Saxer, A.P. Predictions of Three-Dimensional Steady and Unsteady Inviscid Transonic Stator/Rotor Interaction with Inlet Radial Temperature Nonuniformity. *J. Turbomach.* **1994**, *116*, 347–357.
12. Ong, J.; Miller, R.J. Hot Streak and Vane Coolant Migration in a Downstream Rotor. *J. Turbomach.* **2012**, *134*, 051002. [CrossRef]
13. Gaetani, P.; Persico, G.; Dossena, V.; Osnaghi, C. Investigation of the Flow Field in a High-Pressure Turbine Stage for Two Stator-Rotor Axial Gaps—Part I: Three-Dimensional Time-Averaged Flow Field. *J. Turbomach.* **2007**, *129*, 572–579. [CrossRef]
14. Gaetani, P.; Persico, G.; Spinelli., A. Coupled effect of expansion ratio and blade loading on the aerodynamics of a high-pressure gas turbine. *Appl. Sci.* **2017**, *7*, 259. [CrossRef]
15. Persico, G.; Gaetani, P.; Osnaghi, C. A Parametric Study of the Blade Row Interaction in a High Pressure Turbine Stage. *J. Turbomach.* **2009**, *131*, 031006. [CrossRef]
16. Gaetani, P.; Persico, G.; Osnaghi, C. Effects of Axial Gap on the Vane-Rotor Interaction in a Low Aspect Ratio Turbine Stage. *J. Propuls. Power* **2010**, *26*, 325–334. [CrossRef]
17. Persico, G.; Mora, A.; Gaetani, P.; Savini, M. Unsteady Aerodynamics of a Low Aspect Ratio Turbine Stage: Modeling Issues and Flow Physics. *J. Turbomach.* **2012**, *134*, 061030. [CrossRef]
18. Gaetani, P.; Persico, G.; Spinelli, A.; Sandu, C.; Niculescu, F. Entropy wave generator for indirect combustion noise experiments in a high-pressure turbine. In Proceedings of the 2015 11th European Turbomachinery Conference, Madrid, Spain, 23–27 March 2015.

19. Bake, F.; Gaetani, P.; Persico, G.; Neuhaus, L.; Knobloch, K. Indirect Noise Generation in a High Pressure Turbine Stage. In Proceedings of the 22nd AIAA/CEAS Aeroacoustics conference 2016, Lyon, France, 30 May–1 June 2016.
20. Persico, G.; Gaetani, P.; Guardone, A. Design and analysis of new concept fast-response pressure probes. *Meas. Sci. Technol.* **2005**, *16*, 1741–1750. [CrossRef]
21. Persico, G.; Gaetani, P.; Guardone, A. Dynamic calibration of fast-response probes in low-pressure shock tubes. *Meas. Sci. Technol.* **2005**, *16*, 1751–1759. [CrossRef]
22. Gaetani, P.; Persico, G.; Dossena, V.; Osnaghi, C. Investigation of the Flow Field in a High-Pressure Turbine Stage for Two Stator-Rotor Axial Gaps—Part II: Unsteady Flow Field. *J. Turbomach.* **2007**, *129*, 580–590. [CrossRef]